

Redox equilibrium of $\text{Fe}^{3+}/\text{Fe}^{2+}$ and diffusivity of iron in alkali-alkaline earth-silicate glass melts

Ki-Dong Kim* and Sung-Ku Kwon

Department of Materials Science and Engineering, Kunsan National University, Kunsan, Chumbuk 573-701, Korea

The redox behavior and diffusivity of iron were studied in alkali-alkaline earth silicates glass melts by means of square wave voltammetry (SWV). According to voltammograms, the potential of the peak due to $\text{Fe}^{3+}/\text{Fe}^{2+}$ moved towards the negative direction with a temperature decrease and the peak current showed a strong dependence on frequency at constant temperature. The standard enthalpy and entropy determined were 75 kJ/mol and 23 J/molK, respectively. The activation energy for the diffusion of iron was 148 kJ/mol. The redox ratio, $[\text{Fe}^{2+}]/[\text{Fe}^{3+}]$ calculated under the assumption that the melt is in equilibrium with air lay in the range 0.02~0.11. By comparison of the thermodynamic properties and the diffusion coefficient of the present melt with those of other silicate melts cited in the literature, the dependence of the peak potential on alkali concentration and, the relation between the self-diffusion coefficient and viscosity are discussed.

Key words: Iron, Redox, Voltammetry, Diffusivity, Glass melts.

Introduction

Iron in technical glasses is an inevitable component because it exists as a common impurity in natural raw materials such as sand, feldspar, dolomite, calcite etc. Iron in glass melts undergoes the following redox reaction (1) through which electron transfer between Fe^{3+} and Fe^{2+} occurs and electrons are provided or occupied by oxygen during the reaction. Therefore, Fe^{3+} , Fe^{2+} and physically dissolved oxygen are in equilibrium:



The equilibrium constant $K(T)$ described by the activities or the concentrations of the respective species depends on the temperature, the atmosphere and the chemical composition of the melt. The redox equilibrium state of iron ions is hence very much concerned with some properties of the melt and the final glass, especially heat transfer in the infrared region or color of glass products [1].

In the last two decades, voltammetric methods proved to enable the determination of thermodynamic properties and diffusion coefficients of multivalent elements in glass melts. Many studies concerned with redox behaviors of iron ions in various silicate melts have been performed in situ in the molten state by square-wave voltammetry (SWV) and they have offered much thermodynamic [2-11] or diffusion data [13-20] related with the reaction (1) at high temperatures. Nevertheless, for the melts with industrial

compositions consisting of multi-components there have been only two voltammetric studies on iron [10, 11]. Alkali-alkaline earth silicate systems are of great importance for the substrate glass of plasma display panel devices [21-23]. This paper provides a study on the $\text{Fe}^{3+}/\text{Fe}^{2+}$ redox equilibrium and the diffusivity of iron in alkali-alkaline earth silicate glass melts doped with 0.1 mol% Fe_2O_3 .

Experimental Procedure

Preparation of melts

The blank melts with the composition in mol% 69.1SiO₂·0.4Al₂O₃·4.5Na₂O·4.4K₂O·6.5MgO·6.5CaO·5.3SrO·1.1BaO·2.1ZrO₂ and the same melts doped with 0.1 mol% Fe_2O_3 were prepared from high purity chemicals. The glass batches of about 300 g were melted at 1550 °C in an electric furnace. The bubble free melts homogenized by stirring with a Pt/Rh rod were transferred to another electric furnace. While the prepared melts were maintained at 1400 °C in the furnace, the electrodes of an electrochemical cell were dipped into the melts to perform SWV measurements. An electrochemical cell for SWV measurements consists of three electrodes immersed into the melt in a Pt/Rh crucible and a potentiostat (Model 273A, EG&G, USA) connected to a computer. A platinum plate 10 × 20 mm and a platinum wire with a diameter of 1 mm were used as a counter electrode and a working electrode, respectively. The other platinum wire called the reference electrode was connected with O^{2-} conducting Y_2O_3 -stabilized ZrO_2 (YSZ) material which was in contact with the melts and flushed by reference air with a known oxygen partial pressure (P_{O_2} : 0.21bar) during the SWV experiments. A detailed description of the cell construction is given in the literature [11, 12].

*Corresponding author:

Tel : +82-63-469-4737

Fax: +82-63-469-4737

E-mail: kdkim@kunsan.ac.kr

SWV Measurements

SWV is for the measurements of current-potential curves under a controlled potential consisting of base and step potential, i.e. a definite potential varied with time is applied to a working electrode relative to a reference electrode and the resulting current is registered at the counter electrode. The measured current-potential curve, called a voltammogram, gives valuable information on the behavior of the redox species. For example, if the applied potential is enough to allow electron donation or acceptance between redox species as described in reaction (1), the resulting voltammogram reveals a characteristic peak current (I_p). The corresponding potential to I_p in a voltammogram is called the peak potential (E_p) that is equal to the standard potential of the redox pair. Therefore, the equilibrium constant $K(T)$ at temperature T described by using the concentration ($[M^{x+}]$ and $[M^{(x+n)+}]$) of the redox pair and the oxygen equilibrium pressure (P_{O_2}) can be expressed in terms of peak potential, E_p , as following Eq. (2):

$$K(T) = \frac{[M^{x+}] \cdot P_{O_2}^{n/4}}{[M^{(x+n)+}]} = \exp \left[\frac{n \cdot F \cdot E_p}{R_g \cdot T} \right] \quad (2)$$

Here, n is the number of electrons transferred, F is the Faraday constant and R_g is the gas constant. $K(T)$ is also correlated with the standard free enthalpy (ΔG^0), the standard enthalpy (ΔH^0) and the standard entropy (ΔS^0) by the following relationship:

$$-R_g T \ln K(T) = \Delta G^0(T) = \Delta H^0 - T \Delta S^0 = -nFE_p \quad (3)$$

The peak current, I_p , depends on the total concentration (C) of the multivalent ion, the diffusion coefficient (D), the step potential (ΔE) and the pulse time (τ) [24]:

$$I_p = \frac{0.3n^2F^2A \cdot C \cdot \Delta E}{R_g T} \sqrt{\frac{D}{\pi \cdot \tau}} \quad (4)$$

where, A is the surface area of the working electrode, F and R_g have their usual meanings.

During SWV measurements at a given temperature the furnace was switched off to avoid disturbance of the measured signal by the current of the heating elements. SWV measurements in the present study were performed under the following conditions: the range of applied potential and frequency, 0~800 mV and 5~1000 Hz. The final voltammogram of each melt at temperatures ranging from 1400 °C to 1000 °C was obtained by subtracting that of the blank melt from the original recorded voltammogram and analyzed with aid of software.

Results

Fig. 1 shows square wave voltammograms at 100 Hz in the temperature range of 1000~1400 °C recorded in melts doped with 0.1 mol% Fe_2O_3 . One peak due to the reduction of Fe^{3+} to Fe^{2+} (expressed as Fe^{3+}/Fe^{2+}) is shown clearly at high temperature. The corresponding peak potential (E_p),

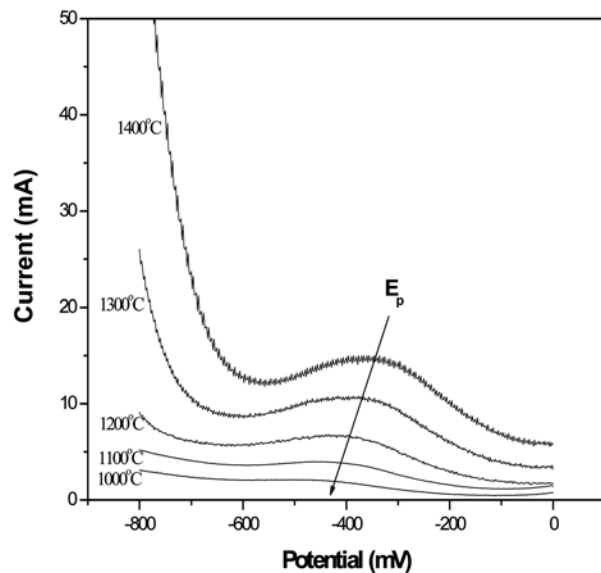


Fig. 1. Voltammograms recorded in alkali-alkaline earth silicate glass melts doped with 0.1 mol% Fe_2O_3 at 100 Hz.

for example -366 mV at 1400 °C moves toward the negative direction with a decrease of temperature as marked by an arrow, indicating that the equilibrium state of reaction (1) shifts towards the left, namely to the oxidation state. In Fig. 2(a) and (b), E_p and $\ln K$ are plotted as a function of temperature, respectively. The temperature dependence in both cases shows a good linearity which means that the reaction enthalpy and entropy are temperature independent in the relevant temperature range.

The redox ratio of iron, $[Fe^{2+}]/[Fe^{3+}]$ in glass melts can be calculated using Eq. (2). Under the assumption that the melt is equilibrated with air ($P_{O_2} = 0.21$ bar), Eq. (2) can be modified to Eq. (5) [25]:

$$\%Fe^{2+} = 100x \frac{[Fe^{2+}]}{[Fe^{2+}] + [Fe^{3+}]} = 100x \frac{K(T)}{K(T) + 0.21^{1/4}} \quad (5)$$

Fig. 3 shows the percentage distribution of Fe^{2+} for the present melt in temperature range of 1000~1400 °C. The percentage of iron in the Fe^{2+} state varies from 2.1% at 1000 °C to 10.4% at 1400 °C. Even though with a temperature increase the equilibrium state of reaction (1) shifts towards to the Fe^{2+} state, its percentage is low absolutely. The converted value of the redox ratio, $[Fe^{2+}]/[Fe^{3+}]$ lies in the range of 0.02~0.11 and is similar to those of other silicate melts [8, 9, 26]. Whereas, the real $[Fe^{2+}]/[Fe^{3+}]$ of commercial glass products in the solid state is within a range of 0.3 to 0.4 [27]. Such a great difference between laboratory melts and industrial glasses must be due to the dependence of the redox ratio on atmosphere and temperature.

In Fig. 4, voltammograms of the present iron-containing melts are shown in the frequency range of 5~1000 Hz at 1300 °C. E_p values at one temperature were independent of frequency, namely the corresponding peak due to Fe^{3+}/Fe^{2+} at 1300 °C is located at -396 mV irrespective

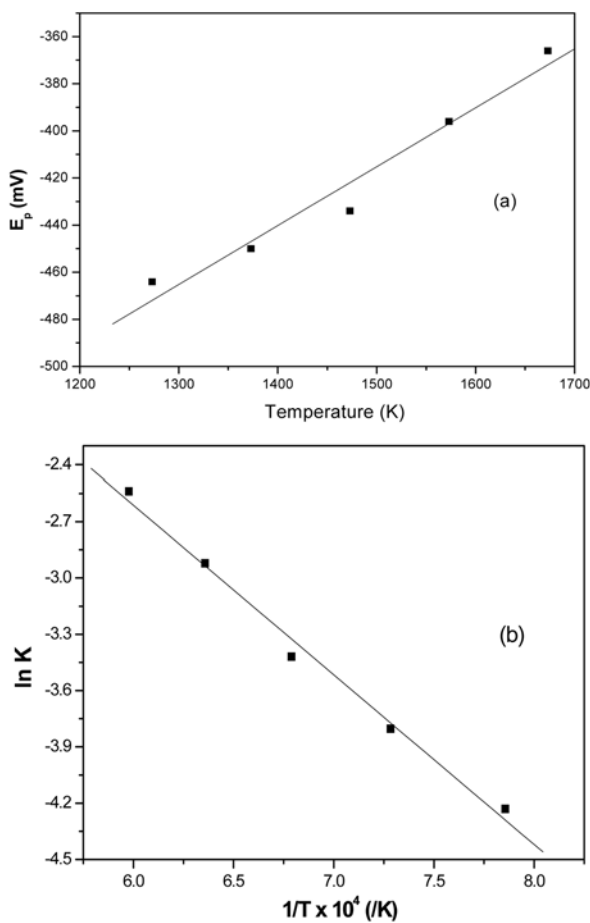


Fig. 2. Experimental plots of (a) peak potential (E_p) and (b) equilibrium constant ($\ln K$) as a function of temperature.

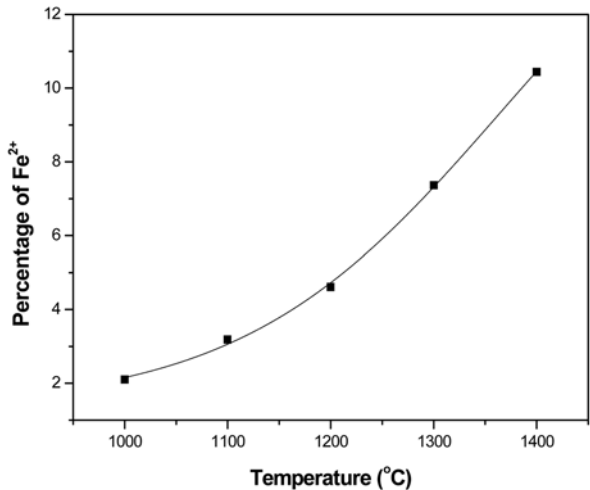


Fig. 3. Percentage of Fe^{2+} as a function of temperature based on equation (5).

of frequency. But the peak currents (I_p) strongly depend on the frequency. For a low frequency such as 5 and 10 Hz, no peak could be observed. However, with an increase in frequency, a peak was observed. According to the relationship between I_p and $\tau^{-1/2}$ as described in Eq. (4), a linear correlation is expected under a diffusion controlled

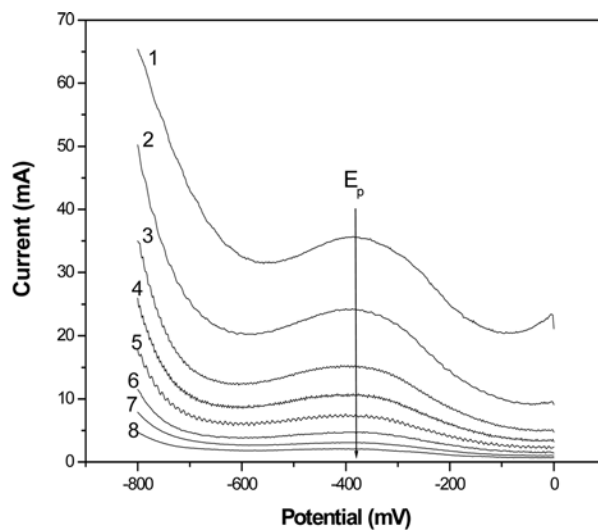


Fig. 4. Voltammograms at 1300 1 : 1000 Hz, 2 : 500 Hz, 3 : 200 Hz, 4 : 100 Hz, 5 : 50 Hz, 6 : 20 Hz, 7 : 10 Hz, 8 : 5 Hz.

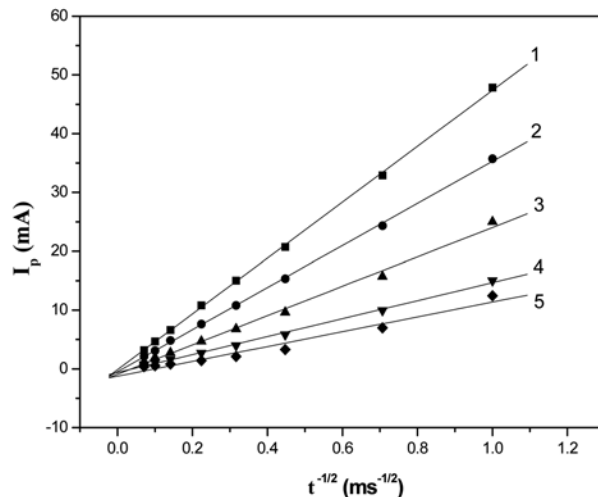


Fig. 5. Peak current (I_p) as a function of $\tau^{-1/2}$ 1 : 1400 °C, 2 : 1300 °C, 3 : 1200 °C, 4 : 1100 °C, 5 : 1000 °C.

reaction. In Fig. 5 I_p is plotted as a function of $\tau^{-1/2}$ at different temperatures and a good linear relation is observed.

Discussion

The thermodynamic data of the $\text{Fe}^{3+}/\text{Fe}^{2+}$ redox reaction were determined from the slope and the interception derived from E_p versus T or $\ln K$ versus $1/T$ based on Eq. (3). The results for E_p at 1300 °C, ΔH^0 and ΔS^0 are summarized in Table 1 inclusive of the data for other silicate melts doped with different iron concentrations. According to some studies [4, 28], the E_p value at one temperature is constant within the limited concentration range of a multivalent element, for example up to 0.5 mol% Fe_2O_3 in alkali lime silicate melts [4]. Therefore, the difference in E_p values of Table 1 is not due to the difference of iron concentration but the different glass compositions. Comparing the data

Table 1. Standard enthalpy (ΔH°) and standard entropy (ΔS°) for the reduction of Fe^{3+}/Fe^{2+} in various silicate melts inclusive of the present melt

Melt code	E_p (mV) at 1300 °C	ΔH° (kJ·mole ⁻¹)	ΔS° (J·mole ⁻¹ ·K ⁻¹)
*Present melt	-396	75	23
A ⁴⁾	-460	102	33
B ^{6, 8)}	-417	83	27
C ⁷⁾	**-520	126	45
E ¹⁰⁾	-392	104	39
F ¹¹⁾	-387	108	45
G ²⁵⁾	-278	79	30

*69.1SiO₂·0.4Al₂O₃·4.5Na₂O·4.4K₂O·6.5MgO·6.5CaO·5.3SrO·1.

1BaO·2.1ZrO₂·0.1Fe₂O₃

**Approximate value read from the figure of reference⁷⁾

A : 74SiO₂·16Na₂O·10CaO·0.1Fe₂O₃

B : 69SiO₂·5Al₂O₃·16Na₂O·10CaO·0.2Fe₂O₃

C : 66.7SiO₂·33.3Na₂O·0.5Fe₂O₃

E : 71.2SiO₂·0.9BaO₃·2.4Al₂O₃·12.5Na₂O·2K₂O·3.8MgO·6.4CaO·

0.8BaO·0.04Fe₂O₃

F : 73.7SiO₂·1.4Al₂O₃·9Na₂O·5K₂O·6SrO·4BaO·0.9ZrO₂·0.07Fe₂O₃

G : 75SiO₂·5Al₂O₃·10Na₂O·10MgO·0.25Fe₂O₃

with the corresponding glass compositions, it seems that E_p , ΔH° and ΔS° are related to the total alkali concentration in melts. In particular, with an increase of alkali concentration E_p moves roughly to a more negative value, for example, E_p of C melt with 33.3Na₂O is expected to be about -520 mV at 1300 °C, E_p for A and B melts with 16Na₂O is -460 mV and -417 mV, E_p of E melt with 14.5(Na₂O + K₂O) and F melt with 14(Na₂O + K₂O) is -392 mV and -387 mV respectively, G melt with 10Na₂O indicates -278 mV and the present melt with 8.9(Na₂O + K₂O) shows -396 mV. This decrease of E_p with an increase of alkali concentration means that the equilibrium state of reaction (1) should be shifted to the left side and thus the Fe^{3+} state is more preferred in the melt. In relation to the dependence of thermodynamic properties on the alkali concentration, it has been suggested based on EPR spectra that with an increase of the alkali concentration the Fe^{2+} state with six fold coordination is changed to the Fe^{3+} state with four fold coordination and

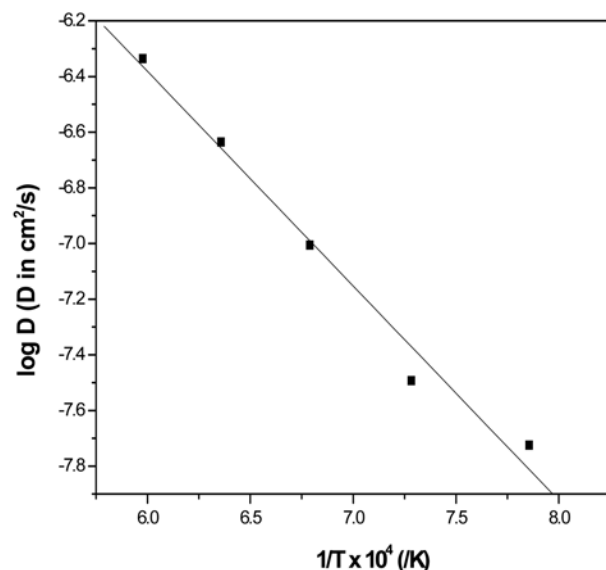


Fig. 6. Temperature dependence of the self-diffusion coefficient (D) for iron ions.

alkali cations participate in charge compensation of $[FeO_4]^-$ tetrahedra [4, 20].

Table 2 contains self-diffusion coefficients (D) of iron calculated from the slope between I_p and $\tau^{-1/2}$ in Fig. 5, and some measured viscosity values (η) of various silicates melts inclusive of the present melt [23]. $\log D$ of the present melt is plotted as a function of $1/T$ in Fig. 6. Within the limits of error, the values can be fitted to an Arrhenius equation, $D = D_0 \exp[-E_D/R_g T]$ where E_D is the activation energy of the self-diffusion process and D_0 the pre-exponential factor. The plot for $\log \eta$ versus $1/T$ also showed Arrhenius behavior in the same temperature range. The calculated activation energy, E_D for diffusion of iron and E_η for viscous flow of the present melt were 148 and 289 kJ/mol, respectively. There have been many studies [14-17, 19] in which the correlation between iron diffusivity and melt viscosity was treated by the Stokes-Einstein equation, $D = kT/6\pi r\eta$, where k is constant and r is the radius of the diffusing species such as iron ion. The results in the literature cited above could be divided into three

Table 2. Self-diffusion coefficient (D : cm²/s) of iron and viscosity (η : dPas) in various silicate melts inclusive of the present melt

Melt code	Temperature (K)				
	1673	1573	1473	1373	1273
Present melt *(η) ²²⁾	$4.619 \times 10^{-7} (10^{2.55})$	$2.315 \times 10^{-7} (10^{3.04})$	$9.869 \times 10^{-8} (10^{3.64})$	$3.220 \times 10^{-8} (10^{4.4})$	$1.885 \times 10^{-8} (10^{5.39})$
A ^{15, 12)}		$1.02 \times 10^{-6} (10^{2.44})$	3.5×10^{-7}		
B ¹⁵⁾		$2.57 \times 10^{-7} (10^{2.82})$			
C ¹⁷⁾		$**1.52 \times 10^{-6}$			1.12×10^{-7}
H ¹³⁾			6×10^{-7}		
I ²⁰⁾		$1.19 \times 10^{-7} (10^{4.28})$			

* Value in parentheses is melt viscosity

**Approximate value read from the figure of reference¹⁷⁾

H : 74SiO₂·26Na₂O·0.2~0.3Fe₂O₃

I : 75SiO₂·5Al₂O₃·5Na₂O·10MgO·5CaO·0.25Fe₂O₃

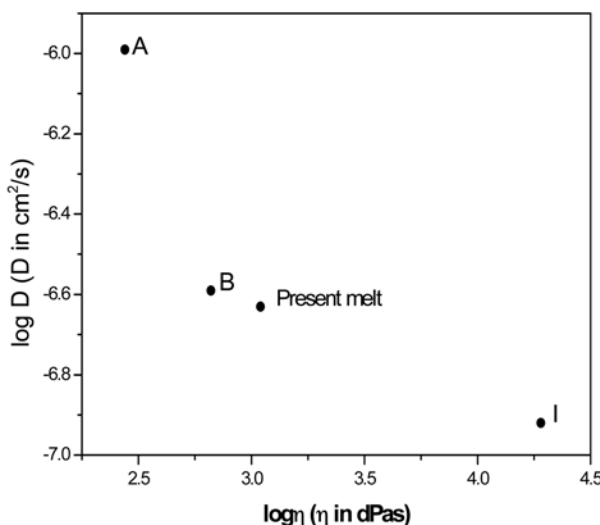


Fig. 7. Plot for the iron self-diffusion coefficient ($\log D$) versus melt viscosity ($\log \eta$) at a constant temperature of 1573 K for four different silicates melts.

categories: 1) the relation between D and $1/\eta$ at constant composition followed the Stokes-Einstein equation, 2) D for different compositions at constant temperature was larger with a smaller η , but showed a deviation from the Stokes-Einstein equation, 3) D for different compositions at constant viscosity was strongly dependent on the glass compositions, for example the concentration and type of alkali oxide. Fig. 7 shows a plot of $\log D$ versus $\log \eta$ at 1573 K for four different silicates melts (A, B, I and the present melt) using the data of Table 2. The smaller η is the larger D is. Thereby, it is expected that the viscosity of melt influences the diffusivity of iron. However, their relation shows a remarkable deviation from the Stokes-Einstein equation as mentioned already in the second category.

Conclusions

Alkali-alkaline earth silicates glass melts, with a composition $69.1\text{SiO}_2\cdot 0.4\text{Al}_2\text{O}_3\cdot 4.5\text{Na}_2\text{O}\cdot 4.4\text{K}_2\text{O}\cdot 6.5\text{MgO}\cdot 6.5\text{CaO}\cdot 5.3\text{SrO}\cdot 1.1\text{BaO}\cdot 2.1\text{ZrO}_2$ doped with 0.1 mol% Fe_2O_3 were studied by the aid of square wave voltammetry. In voltammograms produced in the temperature range of 1000 to 1400 °C and frequency range of 5 to 1000 Hz, there was one reduction peak due to $\text{Fe}^{3+}/\text{Fe}^{2+}$ of which the potential and current depended on the temperature and frequency. The thermodynamic properties for $\text{Fe}^{3+}/\text{Fe}^{2+}$ and the diffusion data of iron in the present melt lay in a similar range to other silicate melts in the literature. However, comparison of the present results with those of other silicate melts indicated that the peak potential decreased with an increase of alkali concentration and the self-diffusion coefficient increased with a decrease of viscosity. In conclusion, glass melts with industrial compositions consisting of multi-components

showed the same behavior in the redox reaction and diffusivity as the simple model glass melts.

Acknowledgement

This work was supported by the Korea Research Foundation (KRF) grant funded by the Ministry of Education, Science and Technology (MEST) (2009-0064154)

References

1. M.B. Volf, "Chemical approach to glass," Elsevier (1984) pp. 347-359
2. E. Freude and C. Rüssel, Glastech. Ber. 63 (1990) 193-197.
3. C. Rüssel and G. Sprachmann, J. Non-Cryst. Solid. 127 (1991) 197-206.
4. C. Rüssel, Glastech. Ber. 66 (1993) 93-99.
5. O. Claussen and C. Rüssel, Glastech. Ber. 69 (1996) 95-100.
6. S. Gerlach, O. Claussen and C. Rüssel, J. Non-Cryst. Solid. 248 (1999) 92-98.
7. C. Rüssel and G. von der Gönna, J. Non-Cryst. Solid. 260 (1999) 147-154.
8. J. de Strycker, S. Gerlach, G. von der Gönna and C. Rüssel, J. Non-Cryst. Solid. 272 (2000) 131-138.
9. G. von der Gönna and C. Rüssel, J. Non-Cryst. Solid. 288 (2001) 175-183.
10. A. Matthai, D. Ehrt and C. Rüssel, Glastech. Ber., Glass Sci. Technol. 73 (2000) 33-38.
11. K.D. Kim and Y.H. Kim, J. Non-Cryst. Solid. 354 (2008) 553-557.
12. K.D. Kim, J. Ceram. Proc. Res. 11 (2010) 25-28.
13. C. Rüssel, J. Non-Cryst. Solid. 134 (1991) 169-175.
14. O. Claussen and C. Rüssel, Solid State Ionics 105 (1998) 289-296.
15. S. Gerlach, O. Claussen and C. Rüssel, J. Non-Cryst. Solid. 226 (1998) 11-18.
16. S. Gerlach, O. Claussen and C. Rüssel, J. Non-Cryst. Solid. 240 (1998) 110-117.
17. O. Claussen, S. Gerlach and C. Rüssel, J. Non-Cryst. Solid. 253 (1999) 76-83.
18. G. von der Gönna and C. Rüssel, J. Non-Cryst. Solid. 261 (2000) 204-210.
19. A. Wiedenroth and C. Rüssel, Phys. Chem. Glasses. 43 (2002) 7-11.
20. C. Rüssel, Glastech. Ber. 66 (1993) 68-75.
21. K.D. Kim and J.H. Hwang, Glastech. Ber., Glass Sci. Technol. 72 (1999) 393-397.
22. K.D. Kim, Glass Technology, 41 (2000) 161-164.
23. K.D. Kim, W.M. Jung, S.K. Kwon and S.Y. Choi, J. Korean Ceram. Soc., 43 (2006) 293-298.
24. J.G. Osteryoung and R.A. Osteryoung, Anal. Chem. 57[1] (1985) 101A-110A.
25. A.W.M. Wondergem-de Best, "Redox Behavior and Fining of Molten Glass," in Ph.D thesis at Technical University Eindhoven Netherlands (1994) pp.180-183.
26. A. Wiedenroth and C. Rüssel, J. Non-Cryst. Solid. 320 (2003) 238-245.
27. C.R. Bamford, "Color Generation and Control in Glass", Elsevier Scientific Publishing Co. (1977) pp.141-164.
28. K.D. Kim, J. Korean Ceram. Soc., 45 (2008) 375-379.